



HAL
open science

A One-sided Exponentially Weighted Moving Average Control Chart for Time Between Events

Fupeng Xie, Philippe Castagliola, Yulong Qiao, Xuelong Hu, Jinsheng Sun

► **To cite this version:**

Fupeng Xie, Philippe Castagliola, Yulong Qiao, Xuelong Hu, Jinsheng Sun. A One-sided Exponentially Weighted Moving Average Control Chart for Time Between Events. *Journal of Applied Statistics*, 2022, 49 (15), pp.3928-3957. 10.1080/02664763.2021.1967894 . hal-03835753

HAL Id: hal-03835753

<https://hal.science/hal-03835753>

Submitted on 1 Nov 2022

HAL is a multi-disciplinary open access archive for the deposit and dissemination of scientific research documents, whether they are published or not. The documents may come from teaching and research institutions in France or abroad, or from public or private research centers.

L'archive ouverte pluridisciplinaire **HAL**, est destinée au dépôt et à la diffusion de documents scientifiques de niveau recherche, publiés ou non, émanant des établissements d'enseignement et de recherche français ou étrangers, des laboratoires publics ou privés.

A One-sided Exponentially Weighted Moving Average Control Chart for Time Between Events

FuPeng Xie^a, Philippe Castagliola^b, YuLong Qiao^a, XueLong Hu^c and JinSheng Sun^a

^aSchool of Automation, Nanjing University of Science and Technology, Nanjing, China; ^bUniversité de Nantes & LS2N UMR CNRS 6004, Nantes, France; ^cSchool of Management, Nanjing University of Posts and Telecommunications, Nanjing, China;

ARTICLE HISTORY

Compiled November 1, 2022

Abstract

Exponentially weighted moving average (EWMA) control charts for time-between-events (TBE) are commonly suggested to monitor high-quality manufacturing processes for the early detection of process deteriorations. In this study, an enhanced one-sided EWMA TBE control chart is developed for rapid detection of increases or decreases in the process mean. The use of the truncation method helps to improve the sensitivity of the proposed scheme in the process mean detection. Moreover, by taking the effects of parameter estimation into account, the proposed scheme with estimated parameters is also investigated in this paper. Both the average run length (ARL) and standard deviation of run length (SDRL) performances of the proposed scheme with known and estimated parameters are studied using the Markov chain method, respectively. Furthermore, an optimal design procedure is developed for the recommended one-sided EWMA TBE chart based on ARL. Numerical results show that the proposed optimal one-sided EWMA TBE chart is more sensitive than the existing optimal one-sided exponential EWMA chart in monitoring both upward and downward mean shifts. Meanwhile, it also performs better than the existing comparative scheme in resisting the effect of the parameter estimation. Finally, two illustrative examples are considered to show the implementation of the recommended one-sided EWMA TBE scheme for simulated and real datasets. For the real dataset of F-16 aircraft, the accident occurrences of F-16 are very low, in which case monitoring the time between two successive F-16 accidents is more efficient than the traditional monitoring schemes. Moreover, the usage of the truncation method makes the proposed one-sided EWMA TBE chart more appropriate for monitoring those two datasets with known shift directions, and the operation of the proposed scheme is simple which does not need to predetermine the reflecting boundary of the existing comparative scheme.

KEYWORDS

Control chart; EWMA; Time-between-events; Markov chain model; Parameter Estimation;

1. Introduction

Statistical process control (SPC) can significantly improve the quality of manufacturing processes. As one of the most primary techniques of SPC, control charts have been extensively adopted in many modern manufacturing industries for enhancing productivity, reducing defects or nonconformities, and detecting deterioration in production process. For several recent studies on the application of control charts, readers may refer to [3, 18, 21, 36]. Nowadays, many kinds of control charts have been developed. The most commonly used Shewhart-type charts are easy to implement and efficient in detecting large magnitude of shifts in the process. Conversely, by taking both the current and past information into account, memory-type charts (like, the exponentially weighted moving average (EWMA) and cumulative sum (CUSUM) charts) are considered as good alternatives to the Shewhart-type scheme in monitoring small to moderate shifts, see [5, 13]. Although traditional control charts have received much attention in the literature, most of these works were based on the assumption that the quality characteristic follows a normal distribution. In fact, this assumption may be not valid in the case of high-quality manufacturing processes, where the occurrences of defects or nonconformities are very low, like, parts per million (ppm). Additionally, there are many problems when one implement a traditional control chart in high-quality manufacturing processes, for instance, high false alarm probability, meaningless control limits and low detection efficiency, see [34]. One effective way to

circumvent these problems is to design TBE (Time-Between-Events) type charts to monitor the time between successive occurrences of a specific event. A common assumption for TBE type charts is that the occurrence of events can be modeled as a homogeneous Poisson process, and the time between two successive events follows an exponential distribution. Based on this assumption, numerous research works on TBE charts have been developed over the years, see for instance [2, 12, 24, 27, 31, 33].

Since the inter-arrival times of defects (or nonconformities) in high-quality manufacturing processes are assumed to be independent and identically distributed (i.i.d.) exponential random variables, some TBE charts can also be named as the exponential control charts (see [9, 35]). Three different types of exponential control charts have already been developed, namely, the exponential Shewhart charts (see [15, 35, 37]), the exponential CUSUM charts (see [8, 24, 25]) and the exponential EWMA charts. Among them, the exponential EWMA charts have received widespread attention due to its high sensitivity in detecting small to moderate shifts. For instance, [9] developed a widely used one- and two-sided exponential EWMA charts for monitoring TBE data. Based on the research in [9], Gan in [10] presented a program for determining the exact average run length (ARL) values of the one- and two-sided exponential EWMA charts, [19] analyzed the effects of parameter estimation on the performance of the one-sided exponential EWMA charts, and [23] developed two optimal design procedures for the one-sided exponential EWMA charts based on median run length (MRL) and expected median run length (EMRL), respectively. Furthermore, it is worth noting that various approaches have been developed in the literature to transform the exponentially distributed data into approximately normal ones, like, the double square root (SQRT) transformation proposed by [16], the weighted standard deviations (WSD) method investigated by [7], and the transformed variable $T^* = T^{1/3.6}$ employed in [4, 14]. Although attractive, data transformations should be considered with care as an appropriate method for high-quality manufacturing processes monitoring, because it may lead to some loss of useful information.

In real application, some situations are so critical that it is only necessary to monitor upward (or downward) shifts of the process. For instance, information on the increase in infection rate of a particular disease (like, the COVID-19) is very important for CDC (Centers for Disease Control) and local governments to adjust epidemic prevention and control measures, because this increase represents an increased risk to the public health. In this context, one-sided type control charts are more appropriate for the processes if the direction of potential mean shift can be anticipated. The one-sided generalized control chart with reflecting boundaries was firstly introduced by [6]. So far, this methodology has been adopted by many researches. For example, [38] proposed a one-sided EWMA chart with reflecting boundaries for monitoring the mean of censored Weibull lifetimes, and [22] investigated the MRL properties of the one-sided exponential EWMA chart with reflecting boundaries (hereafter denoted as the one-sided REWMA chart) when process parameters are estimated. For the one-sided REWMA scheme, both the choice and the effects of using reflecting boundaries on this scheme were investigated in [9]. Moreover, according to [20], the usage of reflecting boundary helps to improve the sensitivity of the scheme for detecting process deteriorations, because the reflecting boundary of the one-sided REWMA chart ensures that the control statistics are at most at a certain distance away from the control limit. Based on these, the one-sided REWMA scheme was often suggested to detect either upward or downward shifts in the case of high-quality manufacturing processes.

Different from the one-sided type scheme with reflecting boundaries, [29] proposed a new improved one-sided EWMA chart using a truncation method for normally distributed data. The basic idea of the truncation method is to accumulate positive (or negative) deviations from the target only, and to truncate negative (or positive) deviations from the target to zero in the computation of the EWMA statistic at each timestep. Comparison results implied that the improved one-sided EWMA scheme performs better than the traditional one-sided EWMA type schemes for monitoring mean shifts in the case of normally distributed processes. Based on the truncation method, [28] proposed a new EWMA dispersion chart by truncating negative normalized observations to zero in the traditional EWMA statistic. Moreover, [30] extended this new “resetting rule” to Poisson processes by using a normalizing transformation, and [11] constructed new one-sided and two one-sided multivariate EWMA schemes for detecting irregular changes in the mean vector of a multivariate normal process. Motivated by the fact that the truncation method proposed by [29] can substantially improve the performance of the one-sided EWMA control chart based on the normal assumption, the goal of this paper is to investigate the efficiency of the truncation method on the one-sided EWMA control chart for TBE data.

The key contributions of this paper can be summarized as follows:

- To propose an enhanced one-sided EWMA TBE control chart using the truncation method for detecting increases or decreases of the process mean.
- To establish a dedicated Markov chain model for evaluating the average run length (ARL) and standard deviation of run length (SDRL) performances of the recommended scheme with known and estimated parameters.
- To develop an optimal design procedure of the proposed one-sided EWMA TBE chart based on ARL.

The outline of this paper is organized as follows: The one-sided EWMA TBE charts with known and estimated parameters are respectively introduced in Section 2. In Section 3, the corresponding Markov chain models are established to investigate the run length (RL) properties (including the ARL and SDRL performances) of the proposed one-sided EWMA TBE schemes with known and estimated parameters. Moreover, an optimal design procedure of the proposed one-sided EWMA TBE chart is developed based on ARL. The existing one-sided REWMA chart is introduced in Section 4 for the comparison with the proposed one-sided EWMA TBE chart. Subsequently, numerical comparisons are performed with the one-sided REWMA charts for both upward and downward shifts. Several guidelines for constructing the one-sided EWMA TBE scheme are also provided. In Section 5, two examples are presented to demonstrate the usage of the proposed one-sided EWMA TBE chart for simulated and real datasets. Finally, Section 6 concludes with some remarks and directions for future researches.

2. Design of the proposed one-sided EWMA TBE chart

2.1. The proposed scheme with known parameters

Let us assume that the TBE random variable X_t used in this paper follows an exponential distribution with scale parameter θ . The probability density function (p.d.f.) $f(x)$ and the corresponding cumulative distribution function (c.d.f.) $F(x)$ of the TBE random variable X_t are $f(x) = \frac{1}{\theta}e^{-\frac{x}{\theta}}$ and $F(x) = 1 - e^{-\frac{x}{\theta}}$, respectively. In order to simplify the design of the proposed one-sided EWMA TBE chart, the scaled TBE random variable $Y_t = X_t/\theta_0$ can be considered (see [19]), where θ_0 is the known in-control scale parameter. Then, if we define $c = \theta/\theta_0$ and $S_t = X_t/\theta$, the scaled TBE random variable Y_t can be restated as,

$$Y_t = \frac{\theta}{\theta_0} \cdot \frac{X_t}{\theta} = c \cdot S_t, \quad (1)$$

where c is a constant that represents the shift level in the in-control scale parameter θ_0 , and the random variable S_t , which denotes the TBE observations X_t scaled with the scale parameter θ , is a standard exponentially distributed random variable with mean 1. The situation where $c > 1$ (or $0 < c < 1$) denotes that an increase (a decrease) in the process parameter θ_0 occurred, and the special case $c = 1$ corresponds to the in-control state.

In this study, the upper-sided EWMA TBE scheme using a truncation method is suggested for quickly detecting upward shifts in the process mean. The basic idea of the proposed truncation method is to truncate the TBE observations X_t below the in-control scale parameter θ_0 to the value of θ_0 , and to only accumulate the TBE observations X_t above the in-control scale parameter θ_0 in the computation of the EWMA recursion. Without loss of generality, the truncation method used in the proposed upper-sided EWMA TBE chart can be achieved by using the upper-truncated TBE random variable defined as follow, i.e.,

$$X_t^+ = \max(\theta_0, X_t). \quad (2)$$

For the scaled TBE random variable Y_t , the upper-truncated TBE random variable can be restated as,

$$Y_t^+ = \max(1, Y_t). \quad (3)$$

When the process is in-control (i.e., $c = 1$), the in-control mean and variance of Y_t^+ are $1 + e^{-1}$ and $e^{-1}(2 - e^{-1})$, respectively (see Appendix A for details). Furthermore, in order to simplify the design, the scaling of

the upper-truncated TBE random variable Y_t^+ is considered as follow,

$$Z_t^+ = \frac{Y_t^+}{1 + e^{-1}}, \quad (4)$$

and then the upper-sided EWMA statistic Q_t^+ can be defined as,

$$Q_t^+ = rZ_t^+ + (1 - r)Q_{t-1}^+, \quad (5)$$

where $r \in (0, 1]$ is a smoothing parameter, and the initial value $Q_0^+ = 1$. The upper-sided EWMA TBE scheme gives an out-of-control signal when $Q_t^+ > H^+$, where H^+ is the control limit of the proposed upper-sided EWMA TBE chart.

Similarly, the recommended lower-sided EWMA TBE scheme is used for quickly monitoring downward shifts in the process mean. The lower-truncated TBE random variable Y_t^- is defined as,

$$Y_t^- = \min(1, Y_t). \quad (6)$$

If $c = 1$, the in-control mean and variance of Y_t^- are $1 - e^{-1}$ and $1 - e^{-1}(2 + e^{-1})$, respectively (see Appendix A for details). Also, the scaling of the lower-truncated TBE random variable Y_t^- is given as follow,

$$Z_t^- = \frac{Y_t^-}{1 - e^{-1}}. \quad (7)$$

Then, the lower-sided EWMA statistic Q_t^- is defined as,

$$Q_t^- = rZ_t^- + (1 - r)Q_{t-1}^-, \quad (8)$$

where the initial value $Q_0^- = 1$. The proposed lower-sided EWMA TBE scheme triggers an out-of-control signal when $Q_t^- < H^-$, where H^- is the control limit of the proposed lower-sided EWMA TBE scheme.

2.2. The proposed scheme with estimated parameters

The one-sided EWMA TBE schemes introduced above are based on the assumption that the in-control scale parameter θ_0 of the exponential distribution is already known. However, process parameters are rarely known in practice, and this fact means that it is necessary to estimate the in-control scale parameter θ_0 using m in-control TBE observations (denoted as X'_1, X'_2, \dots, X'_m) collected in Phase I. The maximum likelihood estimator of θ_0 is defined as (see [39]),

$$\hat{\theta}_0 = \frac{1}{m} \sum_{l=1}^m X'_l. \quad (9)$$

According to [19], the estimated TBE random variable \hat{Y}_t can be obtained by replacing θ_0 in $Y_t = X_t/\theta_0$ with $\hat{\theta}_0$ in (9), i.e.,

$$\hat{Y}_t = \frac{X_t}{\hat{\theta}_0}. \quad (10)$$

Furthermore, let $K = \theta_0/\hat{\theta}_0$, $c = \theta/\theta_0$ and $S_t = X_t/\theta$, and then the estimated TBE random variable \hat{Y}_t in (10) can be restated as,

$$\hat{Y}_t = \frac{\theta_0}{\hat{\theta}_0} \cdot \frac{\theta}{\theta_0} \cdot \frac{X_t}{\theta} = K \cdot c \cdot S_t. \quad (11)$$

Note that the random variable K denotes the ratio of the in-control scale parameter θ_0 to its estimator $\hat{\theta}_0$. It has been proven by [19] that the random variable K follows an inverse gamma distribution and the p.d.f. $f_K(k|m)$ of the random variable K is given as follow,

$$f_K(k|m) = \frac{m^m}{(m-1)!} k^{-m-1} \exp\left(-\frac{m}{k}\right), \quad (12)$$

where m is the number of in-control TBE observations collected in phase I.

Due to the estimation of the in-control scale parameter θ_0 , the corresponding upper- and lower-truncated TBE random variables \hat{Y}_t^+ and \hat{Y}_t^- can also be considered as estimates, say,

$$\hat{Y}_t^+ = \max(1, \hat{Y}_t), \quad (13)$$

$$\hat{Y}_t^- = \min(1, \hat{Y}_t). \quad (14)$$

The in-control mean of \hat{Y}_t^+ and \hat{Y}_t^- are $1 + Ke^{-\frac{1}{K}}$ and $K - Ke^{-\frac{1}{K}}$, respectively (see Appendix A for details). Let $\hat{Z}^+ = \hat{Y}_t^+ / (1 + Ke^{-\frac{1}{K}})$ and $\hat{Z}^- = \hat{Y}_t^- / (K - Ke^{-\frac{1}{K}})$, and then the corresponding upper- and lower-sided EWMA statistics \hat{Q}_t^+ and \hat{Q}_t^- with estimated parameters are defined as follow,

$$\hat{Q}_t^+ = r\hat{Z}_t^+ + (1-r)\hat{Q}_{t-1}^+, \quad (15)$$

$$\hat{Q}_t^- = r\hat{Z}_t^- + (1-r)\hat{Q}_{t-1}^-, \quad (16)$$

where the initial value $\hat{Q}_0^+ = \hat{Q}_0^- = 1$. For the detection of an upward (or a downward) shift of the process mean, the suggested upper-sided (lower-sided) EWMA TBE scheme gives an out-of-control signal when $\hat{Q}_t^+ > \hat{H}^+$ ($\hat{Q}_t^- < \hat{H}^-$), where \hat{H}^+ (\hat{H}^-) is the control limit of the proposed upper-sided (lower-sided) EWMA TBE scheme with estimated parameters.

3. Run length properties of the one-sided EWMA TBE chart

According to [11], the RL properties of a control chart can help practitioners to evaluate the sensitivity of the scheme against shifts of various magnitudes. The average run length (ARL), median run length (MRL) and standard deviation of run length (SDRL) are the three most commonly used RL characteristics for control charts. Due to the space consideration, only the ARL and SDRL performances of the proposed one-sided EWMA TBE chart are investigated in this paper. By definition, the ARL is the average number of TBE observations required for the proposed one-sided EWMA TBE scheme to give a signal. It is expected that the suggested one-sided EWMA TBE scheme runs with a large in-control ARL (hereafter denoted as ARL_0) when the process is in-control ($c = 1$). Conversely, if the process is out-of-control ($c \neq 1$), the proposed one-sided EWMA TBE chart is expected to detect the mean shift quickly, say, a small out-of-control ARL (hereafter denoted as ARL_1) as possible. Besides, according to the definition, the SDRL quantifies the variability of the RL, and the smaller the SDRL, the better the RL performance of a control chart.

3.1. A Markov chain model for the proposed scheme

Generally, the RL properties of EWMA type control charts are evaluated using integral equations, Markov chain methods or Monte Carlo simulations. In this paper, a Markov chain model is established to evaluate the ARL and SDRL performances of the proposed one-sided EWMA TBE charts with known and estimated parameters. Without loss of generality, every states of the Markov chain are defined by partitioning the in-control region into M subintervals (labeled as $i = 1, 2, \dots, M$). The midpoint value within each sub-interval is suggested to approximate the value of the corresponding one-sided EWMA statistic. For the known parameter case, the RL of the one-sided EWMA TBE chart is a Discrete Phase-type (DPH) random variable of

parameters (\mathbf{Q}, \mathbf{p}) , where the transition probability matrix \mathbf{Q} is

$$\mathbf{Q} = \begin{pmatrix} q_{1,1} & q_{1,2} & \cdots & q_{1,M} \\ q_{2,1} & q_{2,2} & \cdots & q_{2,M} \\ \vdots & \vdots & \ddots & \vdots \\ q_{M,1} & q_{M,2} & \cdots & q_{M,M} \end{pmatrix}, \quad (17)$$

and \mathbf{p} is the initial probabilities associated with the M transient states, say, $\mathbf{p} = (p_1, p_2, \dots, p_M)^\top$.

Taking the proposed upper-sided EWMA TBE chart with known parameters as an example, the mean and variance of the variable $Y_t^+ = \max(1, Y_t)$ are $1 + e^{-1}$ and $e^{-1}(2 - e^{-1})$, respectively. Because of (4), it is easy to obtain that the upper-sided EWMA statistic $Q_t^+ = rZ_t^+ + (1 - r)Q_{t-1}^+ \geq \frac{1}{1+e^{-1}}$, and then divide the in-control region $[\frac{1}{1+e^{-1}}, H^+]$ into M subintervals of width $w^+ = \frac{H^+ - 1/(1+e^{-1})}{M}$ to obtain a discretized Markov chain model. The charting statistic Q_t^+ is considered to be in transient state i , at time t , if $L_i^+ - \frac{w^+}{2} < Q_t^+ \leq L_i^+ + \frac{w^+}{2}$, where $L_i^+ = \frac{1}{1+e^{-1}} + (i - 0.5)w^+$ is the midpoint value of the i th subinterval. If we define the element $q_{i,j}$ to be the transition probability of statistic Q_t^+ from state i to state j . Then,

$$\begin{aligned} q_{i,j} &= \Pr(Q_t^+ \in \text{state } j \mid Q_{t-1}^+ \in \text{state } i) \\ &= \Pr\left(L_j^+ - \frac{w^+}{2} < Q_t^+ \leq L_j^+ + \frac{w^+}{2} \mid Q_{t-1}^+ = L_i^+\right) \end{aligned} \quad (18)$$

After some algebraic operations, the element $q_{i,j}$ is equal to,

$$\begin{aligned} q_{i,j} &= \Pr\left(\frac{1}{1+e^{-1}} + \frac{[j-1 - (1-r)(i-0.5)]w^+}{r} \right. \\ &\quad \left. < Z_t^+ \leq \frac{1}{1+e^{-1}} + \frac{[j - (1-r)(i-0.5)]w^+}{r}\right) \\ &= \Pr\left(1 + \frac{(1+e^{-1})[j-1 - (1-r)(i-0.5)]w^+}{r} \right. \\ &\quad \left. < Y_t^+ \leq 1 + \frac{(1+e^{-1})[j - (1-r)(i-0.5)]w^+}{r}\right) \end{aligned} \quad (19)$$

Furthermore, let us define,

$$A_1 = 1 + \frac{(1+e^{-1})[j-1 - (1-r)(i-0.5)]w^+}{r}, \quad (20)$$

$$A_2 = 1 + \frac{(1+e^{-1})[j - (1-r)(i-0.5)]w^+}{r}. \quad (21)$$

Then, the entire $q_{i,j}$ in the transition probability matrix \mathbf{Q} can be computed as follow,

$$q_{i,j} = \begin{cases} 0, & \text{if } A_2 < 1 \\ F_S\left(\frac{A_2}{c}\right), & \text{if } A_2 \geq 1 \text{ and } A_1 < 1 \\ F_S\left(\frac{A_2}{c}\right) - F_S\left(\frac{A_1}{c}\right), & \text{if } A_2 \geq 1 \text{ and } A_1 \geq 1 \end{cases} \quad (22)$$

where $F_S(s) = 1 - e^{-s}$ is the c.d.f. of the standard exponentially distributed random variable S_t defined in

(1). In addition, the elements p_j of vector \mathbf{p} are,

$$p_j = \begin{cases} 1, & L_j^+ - \frac{w^+}{2} < Q_0^+ < L_j^+ + \frac{w^+}{2} \\ 0, & \text{otherwise} \end{cases} \quad (23)$$

where $Q_0^+ = 1$. Finally, the ARL and SDRL values of the proposed one-sided EWMA TBE chart with known parameters can be computed as follow,

$$\text{ARL} = \mathbf{p}^\top (\mathbf{I} - \mathbf{Q})^{-1} \mathbf{1}, \quad (24)$$

$$\text{SDRL} = \sqrt{2\mathbf{p}^\top (\mathbf{I} - \mathbf{Q})^{-2} \mathbf{Q} \mathbf{1} - (\text{ARL})^2 + \text{ARL}}, \quad (25)$$

where $\mathbf{1}$ is a $(M, 1)$ vector of 1's, and \mathbf{I} is the (M, M) identity matrix. For more details about the Markov chain model of the lower-sided EWMA TBE chart and their corresponding estimated parameter counterparts, please see Appendix B.

3.2. Optimal design procedure of the proposed scheme

For the suggested one-sided EWMA TBE scheme, once the number M of the subintervals, and the smoothing parameter r of the scheme are fixed, an approximated value of H can be easily obtained by imposing the constraint that the acceptable ARL_0 should attain the pre-specified target. In this paper, the number $M = 500$ of the subintervals are selected, and the corresponding steps for searching H of the upper-sided EWMA TBE scheme are given as follow:

Step 1: Set the values of ARL_0 , M , r , and $c = 1$;

Step 2: Let H have the initial value of $1/(1 + e^{-1})$;

Step 3: Compute the ARL_0 value using (24);

Step 4: If $\text{ARL}_0 \geq 200.1$ (or $\text{ARL}_0 \leq 199.9$), let $H = H - 0.0001$ ($H = H + 0.0001$), and then go to Step 3. Otherwise, when $\text{ARL}_0 \in [199.9, 200.1]$, control flow moves to the next step.

Step 5: Stop searching and the current value of H is recorded.

The optimal design of the one-sided EWMA TBE scheme aims at finding the proposed one-sided EWMA TBE chart having the minimum ARL_1 (denoted as ARL_{opt}) value for the specified mean shift c_{opt} , among the schemes with the desired ARL_0 value. In view of this, the optimal procedure can be modeled as a nonlinear minimization problem. Due to the space limitation, only the optimal procedure of the proposed one-sided EWMA TBE scheme with known parameters is given for illustration, i.e.,

$$(r^*, H^*) = \underset{(r, H)}{\text{argmin}} \text{ARL}_1(r, H, c_{\text{opt}}). \quad (26)$$

Subject to

$$\text{ARL}(r^*, H^*, c_{\text{opt}} = 1) = \text{ARL}_0, \quad (27)$$

where r and H represent the smoothing parameter and the control limit of the proposed one-sided EWMA TBE chart, respectively. Meanwhile, (r^*, H^*) is the optimal parameter combination of the proposed one-sided EWMA TBE scheme with known parameters for a fixed mean shift c_{opt} .

The optimal parameter combination (r^*, H^*) of the proposed one-sided EWMA TBE chart can be obtained using (26) and (27) when ARL_0 and c_{opt} are specified. Without loss of generality, the optimal procedure is summarized as follow:

Step 1: Set the values of the desired ARL_0 and the mean shift c_{opt} ;

Step 2: Initialize the smoothing parameter $r = 0.01$;

Step 3: With the constraint on the desired ARL_0 specified in Step 1, find the control limit H for the corresponding r ;

Step 4: Compute the ARL_1 value for the corresponding combination (r, H) determined in Step 3 and the mean shift c_{opt} specified in Step 1.

Step 5: Repeat Steps 3 and 4 for all values of r varying from 0.01 to 0.99 with a step size 0.0001.

Step 6: The combination (r, H) that produces the ARL_{opt} value for the specified c_{opt} is recorded as the optimal parameter combination (r^*, H^*) of the proposed one-sided EWMA TBE chart.

Similar to [17] and [26], the steps for searching the optimal parameter combination (\hat{r}^*, \hat{H}^*) of the proposed one-sided EWMA TBE chart with estimated parameters are similar to the case with known parameters, except that the number m of in-control TBE observations collected in phase I should be fixed first. After that, for a specified c_{opt} , adjust the control limit \hat{H} of the scheme with the optimal smoothing parameter r^* determined in known parameter case so that the control chart can produce the desired \widehat{ARL}_0 . Then, the optimal parameter combination (\hat{r}^*, \hat{H}^*) and \widehat{ARL}_{opt} (i.e., the minimum \widehat{ARL}_1 value of the proposed one-sided EWMA TBE chart with estimated parameters) for c_{opt} can be obtained.

4. Comparative studies

4.1. The existing one-sided exponential EWMA chart

The one-sided exponential EWMA chart with reflecting boundaries (also named as the one-sided REWMA chart) was firstly introduced by [9] for detecting either increases or decreases in the process mean. In the case of high-quality manufacturing processes, the existing upper-sided REWMA chart is considered when only the upward mean shifts need to be detected. The charting statistic Q_t of the upper-sided REWMA chart can be written as follow:

$$Q_t = \max\{A, \lambda_Q Y_t + (1 - \lambda_Q)Q_{t-1}\}, \quad (28)$$

where A is a reflecting boundary of the existing upper-sided REWMA chart. As suggested by [9], the reflecting boundary A is commonly set as 1 to improve the worst-case RL properties. Besides, the initial value $Q_0 = 1$, and $\lambda_Q \in (0, 1]$ is a smoothing parameter of the existing upper-sided REWMA scheme. An out-of-control signal is generated when Q_t exceeds the control limit h_Q of the existing upper-sided REWMA scheme.

Similarly, the charting statistic q_t of the existing lower-sided REWMA scheme is defined as follow:

$$q_t = \min\{B, \lambda_q Y_t + (1 - \lambda_q)q_{t-1}\}, \quad (29)$$

where B is a lower-sided reflecting boundary and $\lambda_q \in (0, 1]$ is a smoothing parameter of the existing lower-sided REWMA chart. It is also recommended by [9] that $B = 1$ can be used for improving worst-case RL properties of the lower-sided REWMA scheme. In this paper, the initial value $q_0 = 1$, and the existing lower-sided REWMA scheme signals if q_t is smaller than the control limit h_q of the existing lower-sided REWMA scheme.

Although the corresponding integral equations have been derived by [9] for computing the ARL value of the existing one-sided REWMA chart, the Markov chain model is also popular and used in this paper for evaluating the RL properties of the existing one-sided REWMA chart so as to keep consistency with the proposed one-sided EWMA TBE scheme. For more details about the Markov chain method of the existing one-sided REWMA chart, readers can refer to [23]. Furthermore, the existing one-sided REWMA chart is compared with the proposed one-sided EWMA TBE chart in both the known and the estimated parameter cases. With the same ARL_0 , the control chart, which produces a smaller out-of-control ARL value, is considered to be more sensitive for the fixed mean shift c .

4.2. Comparison under upward shifts

As mentioned in [32], an event in a process can be classified into two categories: the negative or the positive. A negative event may be a quality problem, a natural disaster or an epidemic outbreak in real applications.

On the contrary, the purchase order of a product, the success of an activity, the profit in a business, etc., may be considered positive events. For a high-quality process, the upward shift detection is very important when the events we are interested in are positive ones. For example, a store manager should pay attention to monitor a downward shift in the purchase order, because the decrease in the purchase order of a particular product means that this product may be overstocked in the future.

In order to evaluate the ARL and SDRL performances of the proposed upper-sided EWMA TBE scheme for upward mean shifts, the control limits H^+ and \widehat{H}^+ of the proposed upper-sided EWMA TBE schemes with known and estimated parameters are respectively listed in Table 1, for different desired $ARL_0 \in \{200, 370, 500\}$ and different values of $m \in \{10, 50, 200, +\infty\}$ when the smoothing parameter r ranges from 0.03 to 0.90. It is noted that $m = +\infty$ corresponds to the known parameter case. Additionally, with the same settings, the control limits h_Q and \widehat{h}_Q of the existing upper-sided REWMA schemes for the known and estimated parameter cases are also presented in Table 1, respectively. It can be seen from Table 1 that, for a specified r and ARL_0 , the \widehat{H}^+ value of the proposed upper-sided EWMA TBE chart with estimated parameters tends to be closer to its known parameter counterpart H^+ , as m increases. This means that the effect of estimated parameters on the performance of the proposed scheme is large when the number of Phase I TBE observations m is small.

(Please insert Table 1 here)

The ARL (\widehat{ARL}) and SDRL (\widehat{SDRL}) values of the proposed upper-sided EWMA TBE chart with known (estimated) parameters can be obtained using the Markov chain model provided in Section 3.1. Owing to space limitation, for the known parameter case, only the ARL_1 and $SDRL_1$ values with the constraint on the desired $ARL_0 = 500$ are presented in Table 2. For instance, when the smoothing parameter $r = 0.05$ and the upward mean shift $c = 1.3$, the ARL_1 and $SDRL_1$ of the proposed upper-sided EWMA TBE scheme are 53.81 and 46.07, respectively. Meanwhile, the corresponding ARL_1 and $SDRL_1$ of the existing upper-sided REWMA chart are 58.65 and 49.14, respectively. In addition, for the parameter estimation case, the \widehat{ARL}_1 and \widehat{SDRL}_1 values of the proposed and existing upper-sided EWMA type schemes are respectively presented in Table 3, based on the Phase I TBE observations $m = 200$ and $\widehat{ARL}_0 = 500$. For example, when the upward mean shift $c = 2$ and the smoothing parameter $r = 0.3$, the \widehat{ARL}_1 and \widehat{SDRL}_1 of the proposed upper-sided EWMA TBE scheme are 14.93 and 13.48, respectively. Meanwhile, the corresponding \widehat{ARL}_1 and \widehat{SDRL}_1 of the existing upper-sided REWMA chart are 15.00 and 13.39, respectively.

(Please insert Tables 2 and 3 here)

Several conclusions can be drawn from Tables 2 and 3 that,

- For the same smoothing parameters (i.e., $r = \lambda_Q$), the suggested upper-sided EWMA TBE scheme with known parameters is uniformly more sensitive than the corresponding upper-sided REWMA scheme in detecting the whole upward shift domain. On the other hand, for the estimated parameter case (i.e., $m = 200$), the proposed upper-sided EWMA TBE scheme is superior to the upper-sided REWMA scheme, when only a small smoothing parameters (say, $r < 0.5$) is selected.
- For a fixed upward mean shift c , the ARL_1 and $SDRL_1$ performances of the proposed upper-sided EWMA TBE scheme and the existing upper-sided REWMA scheme tend to be similar as the smoothing parameter r increases. For instance, when upward mean shift $c = 1.1$ and $r = 0.05$, the $(ARL_1, SDRL_1)$ values of the upper-sided EWMA TBE chart and the upper-sided REWMA chart are (178.36, 170.61) and (191.67, 180.90), respectively. Meanwhile, with the same $c = 1.1$, the corresponding $(ARL_1, SDRL_1)$ values of these two schemes for $r = 0.8$ are (279.67, 279.13) and (279.96, 279.36), respectively.
- Compared with the upper-sided REWMA scheme, the effect of the parameter estimation on the recommended upper-sided EWMA TBE scheme is relatively small. It can be observed that there is a small difference between the $(ARL_1, SDRL_1)$ and $(\widehat{ARL}_1, \widehat{SDRL}_1)$ values of the proposed upper-sided EWMA TBE chart. Conversely, the corresponding difference between $(ARL_1, SDRL_1)$ and $(\widehat{ARL}_1, \widehat{SDRL}_1)$ values of the existing upper-sided REWMA chart is clear, especially for a small smoothing parameter. This fact implies that the proposed upper-sided EWMA TBE chart is more effective than the upper-sided REWMA chart in resisting the effect of parameter estimation.

The optimal parameter combinations (r^*, H^{+*}) and (λ_Q^*, h_Q^*) of the proposed upper-sided EWMA TBE chart and the upper-sided REWMA chart for different upward mean shifts c_{opt} are respectively given in Table 4. Meanwhile, the corresponding ARL_{opt} and ARL'_{opt} of these two charts are also provided, respectively. For instance, when the upward mean shift $c_{\text{opt}} = 2$, the optimal parameter combination (r^*, H^{+*}) and ARL_{opt} of the recommended upper-sided EWMA TBE scheme are (0.06, 1.2922) and 12.1483, respectively, and the corresponding optimal parameter combination (λ_Q^*, h_Q^*) and ARL'_{opt} of the existing upper-sided REWMA chart are (0.0872, 1.7077) and 13.1082, respectively. It can be made from Table 4 that, for a specified ARL_0 , the optimal smoothing parameter r^* of the recommended upper-sided EWMA TBE scheme increases, as the upward mean shift c_{opt} increases. Moreover, it can be observed that the optimal upper-sided EWMA TBE chart is superior to the optimal upper-sided REWMA chart in the whole upward shift domain, especially for small upward mean shifts c_{opt} . In order to make a quantitative assessment of the ARL_{opt} values, the average of the ratio (AR) of ARL_{opt} to ARL'_{opt} is defined as,

$$\text{AR} = \frac{1}{N} \sum_{J=1}^N \frac{\text{ARL}_{\text{opt}}(c_{\text{opt},J})}{\text{ARL}'_{\text{opt}}(c_{\text{opt},J})}, \quad (30)$$

where N is the number of mean shift c_{opt} used in the comparison, $\text{ARL}_{\text{opt}}(c_{\text{opt},J})$ is the minimum ARL_1 value produced by the recommended one-sided EWMA TBE chart at the J th mean shift $c_{\text{opt},J}$, and $\text{ARL}'_{\text{opt}}(c_{\text{opt},J})$ is the minimum ARL'_1 value of the existing one-sided REWMA chart at the same mean shift level. Obviously, if the AR value is smaller than one, the optimal upper-sided (lower-sided) EWMA TBE chart is considered to perform better than the optimal upper-sided (lower-sided) REWMA chart for the pre-specified upward (downward) shift domain and *vice versa*. As it can be computed in Table 4, the AR value of the proposed optimal upper-sided EWMA TBE scheme with known parameters is 0.9253 for the upward mean shift domain $c_{\text{opt}} \in \{1.05, 1.2, 1.4, 1.6, 1.8, 2, 3, 4, 5, 6, 7, 8\}$.

(Please insert Table 4 here)

To sum up, irrespective of the known or the estimated parameter case, the proposed upper-sided EWMA TBE scheme with a small smoothing parameter outperforms the corresponding upper-sided REWMA chart for detecting upward shifts in the process mean. Moreover, the proposed upper-sided EWMA TBE chart is more effective than the upper-sided REWMA chart in resisting the effect of parameter estimation.

4.3. Comparison under downward shifts

The downward shift detection is critical when the events we are interested in are negative ones. For example, a decrease in the time between two quality problems of a product indicates that the quality of this product has declined. With the same settings as in the upward shift detection case, the control limits H^- and \hat{H}^- of the proposed lower-sided EWMA TBE schemes with known and estimated parameters are presented in Table 5, respectively. Similar to the upward shift detection case, for a specified r and ARL_0 , the \hat{H}^- value of the proposed lower-sided EWMA TBE scheme with estimated parameters tends to be closer to its known parameter counterpart H^- , as m increases. This also means that the effect of estimated parameter on the in-control ARL performance is large when a small number of Phase I TBE observation m is considered.

(Please insert Table 5 here)

The $\widehat{\text{ARL}}$ and $\widehat{\text{SDRL}}$ performances of the proposed lower-sided EWMA TBE chart with known (estimated) parameters can be obtained using the Markov chain model provided in Appendix B. For comparison, the ARL_1 and SDRL_1 values of the proposed lower-sided EWMA TBE and the existing lower-sided REWMA charts with known parameters are respectively presented in Table 6. For instance, when the smoothing parameter $r = 0.2$ and the downward mean shift $c = 0.3$, the ARL_1 and SDRL_1 of the proposed lower-sided EWMA TBE chart are 9.61 and 4.68, respectively. Meanwhile, the corresponding ARL_1 and SDRL_1 of the existing lower-sided REWMA chart are 10.49 and 3.71, respectively. In addition, for the parameter estimated case, the $\widehat{\text{ARL}}_1$ and $\widehat{\text{SDRL}}_1$ values of the lower-sided EWMA TBE and the lower-sided REWMA charts are presented in Table 7, respectively. For instance, when the smoothing parameter $r = 0.4$ and the downward mean shift $c = 0.2$, the $\widehat{\text{ARL}}_1$ and $\widehat{\text{SDRL}}_1$ values of the proposed lower-sided EWMA TBE chart are 6.91 and 3.46, respectively. And the corresponding $\widehat{\text{ARL}}_1$ and $\widehat{\text{SDRL}}_1$ values of the existing

lower-sided REWMA chart are 7.43 and 3.06, respectively.

(Please insert Tables 6 and 7 here)

It can be concluded from Tables 6 and 7 that,

- Irrespective of the known or the estimated parameter case, the proposed lower-sided EWMA TBE scheme with a small smoothing parameter is superior to the corresponding lower-sided REWMA scheme in monitoring moderate-to-large downward mean shifts.
- For a specified downward mean shift c , the lower-sided EWMA TBE chart and the lower-sided REWMA chart tend to be similar in the ARL_1 and $SDRL_1$ performances with the increase of the smoothing parameter r , especially in the estimated parameter case.
- Similar to the upward shift detection case, the proposed lower-sided EWMA TBE scheme is also performs better than the lower-sided REWMA chart in resisting the effect of parameter estimation.

In order to obtain the ARL_{opt} and ARL'_{opt} values of the proposed lower-sided EWMA TBE chart and the existing lower-sided REWMA chart for different downward mean shifts c_{opt} , the optimal parameter combinations (r^*, H^{-*}) and (λ_q^*, h_q^*) of these two schemes are provided in Table 8, respectively. Based on the ARL_{opt} and ARL'_{opt} values presented in Table 8, the AR value of the proposed lower-sided EWMA TBE chart is 0.9377 for the downward mean shift domain $c_{opt} \in \{0.95, 0.92, 0.9, 0.8, 0.7, 0.6, 0.5, 0.4, 0.3, 0.2, 0.1, 0.05\}$.

(Please insert Table 8 here)

It can also be found in Table 8 that, for a specified ARL_0 , the optimal smoothing parameter r^* of the proposed lower-sided EWMA TBE chart increases, as the downward mean shift c_{opt} decreases. Additionally, the optimal lower-sided EWMA TBE chart is uniformly more effective than the optimal lower-sided REWMA chart in the whole downward shift domain, especially for detecting small downward mean shifts c_{opt} .

5. Examples

To explain the implementation of the recommended one-sided EWMA TBE scheme in monitoring mean shifts of the high-quality processes, a common practice is to consider either a simulated or a real dataset. In this section, two examples are introduced, one with simulated data and the other one with real data from the Hellenic Air Force (HAF) as reported in [1], and then the proposed one-sided EWMA TBE schemes are implemented using these two datasets.

5.1. Example 1

For a high-quality manufacturing process, assume that the time between two successive events follows an exponential distribution with scale parameter $\theta = 10$, i.e., the in-control mean θ_0 of the process is 10. In this example, we generate 30 TBE observations with the parameter $\theta_1 = 18$, see Column 2 in Table 9. The simulated dataset can be viewed as TBE observations from an out-of-control process where the shift is $c = \theta_1/\theta_0 = 1.8$. In order to monitor the upward mean shift more effectively, the proposed upper-sided EWMA TBE scheme is implemented. According to the truncation method given in Section 2.1, all 30 TBE observations X_t were divided by $\theta_0 = 10$ to obtain the scaled TBE observations Y_t . Furthermore, transforming these 30 scaled TBE observations Y_t to the upper-truncated TBE observations Y_t^+ using (3), and then the corresponding upper-sided EWMA statistic Q_t^+ can be obtained, see Column 4 in Table 9. When the upper-sided EWMA statistic Q_t^+ exceeds H^+ , the proposed upper-sided EWMA TBE chart triggers an out-of-control signal, and then the potential assignable causes should be found and removed.

(Please insert Table 9 and Figure 1 here)

To provide a fair comparison with the existing upper-sided REWMA chart, the same smoothing parameter, say, $r = \lambda_Q = 0.1$, is specified in the proposed upper-sided EWMA TBE scheme. Then, with the constraint on $ARL_0 = 200$, the control limits H^+ and h_Q of the upper-sided EWMA TBE chart and the upper-sided REWMA chart are 1.8406 and 1.6460, respectively. The monitoring procedures of these two charts are shown in Figure 1, respectively. Note that the suggested upper-sided EWMA TBE scheme gives an out-of-control signal at the 11th TBE observation, while the existing upper-sided REWMA chart signals at the 16th TBE

observation (both of these two charting statistics are bolded in Table 9). In this example, this represents that the suggested upper-sided EWMA TBE scheme is superior to the existing upper-sided REWMA scheme for monitoring an upward shift.

5.2. Example 2

The real dataset employed in this subsection is related to F-16 aircraft accidents of the Hellenic Air Force (HAF), which was firstly introduced by [1]. The time between two accidents of F-16 aircraft can be regarded as an important quality characteristic for reliability monitoring. In this real dataset, 16 time intervals between consecutive accidents of F-16 aircraft are included, see Column 2 in Table 10. According to [1], it has been proved that the time between accidents of F-16 aircraft from 1 December 1988 to 31 December 2017 fits the gamma distribution with shape parameter $\gamma = 1$ and scale parameter $\theta = 615$ (days). Since the exponential distribution with mean θ is the special case of the gamma distribution with the shape parameter 1 and the scale parameter θ , this means that the time between two successive accidents of F-16 aircraft follows an exponential distribution with scale parameter $\theta_1 = 615$ (days). Furthermore, it is assumed that the in-control value of θ_0 is 1460 (days), i.e., the process is acceptable if an accident occurs every four years. Then, the proposed one-sided EWMA TBE chart can be implemented to monitor those 16 Phase II observations.

(Please insert Table 10 and Figure 2 here)

In order to monitor the process, the same smoothing parameters, say, $r = \lambda_q = 0.03$, are selected. Then, with the constraint on the desired $ARL_0 = 370$, the control limits H^- and h_q of the lower-sided EWMA TBE scheme and the lower-sided REWMA scheme are 0.5462 and 0.7539, respectively. Based on these design parameters, the charting statistics Q_t^- and q_t of these two charts can be obtained, respectively (see Columns 4 and 6 in Table 10). The monitoring procedures of these two charts for the time intervals between consecutive accidents of F-16 aircraft are presented in Figure 2, respectively. As shown in Figure 2, the proposed lower-sided EWMA TBE chart gives an out-of-control signal at the 16th TBE observation, while the existing lower-sided REWMA chart cannot detect the shift at all. This means that the suggested lower-sided EWMA TBE scheme in this example works better than the existing lower-sided REWMA scheme in monitoring a downward shift.

6. Conclusion

This paper investigates a one-sided EWMA TBE scheme using the truncation method for detecting either upward or downward mean shifts. The basic idea of the truncation method is to truncate the TBE observations below (or above) the scale parameter θ to the value of θ , and to accumulate the TBE observations above (or below) the scale parameter θ only. A dedicated Markov chain method has been established to analyze the ARL and SDRL performances of the proposed one-sided EWMA TBE chart with known and estimated parameters. In addition, the optimal design of the proposed one-sided EWMA TBE chart is also provided in this paper. Comparison results demonstrate that the optimal one-sided EWMA TBE chart always outperforms the optimal one-sided REWMA chart in terms of the overall detection effectiveness. Meanwhile, the one-sided EWMA TBE chart performs better than the one-sided REWMA chart in resisting the influence of parameter estimation. More importantly, the operation of the recommended one-sided EWMA TBE scheme is not only as simple as that of the existing one-sided REWMA chart, but also does not need to predetermine the value of reflecting boundary. This means the easy-to-implement one-sided EWMA TBE chart may be a good alternative to the one-sided REWMA chart in monitoring the exponentially distributed data.

In real applications, the steady-state and the worst-case scenarios of a control chart are more informative than its zero-state counterpart. A possible future extension of the current study is to investigate the RL properties (including the ARL, MRL and SDRL) of the proposed one-sided EWMA TBE chart in both the steady-state and the worst-case scenarios. Besides, using a one-sided type chart with the truncation method to monitor the other suitable distributed data (like, Poisson and gamma) for high-quality manufacturing processes could also be considered.

Disclosure statement

No potential conflict of interest was reported by the author(s).

Funding

This work was supported by National Natural Science Foundation of China (Grant number: 71802110, 71671093); Humanity and Social Science Foundation of Ministry of Education of China (Grant number: 19YJA630061); China Scholarship Council (Grant number: 202006840086); Postgraduate Research & Practice Innovation Program of Jiangsu Province (Grant number: KYCX21_0306); Key Research Base of Philosophy and Social Sciences in Jiangsu Information Industry Integration Innovation and Emergency Management Research Center; The Excellent Innovation Teams of Philosophy and Social Science in Jiangsu Province (2017ZSTD022).

References

- [1] V. Alevizakos and C. Koukouvinos, *A double exponentially weighted moving average chart for time between events*, Communications in Statistics-Simulation and Computation 49 (2020), pp. 2765–2784.
- [2] V. Alevizakos, C. Koukouvinos, and A. Lappa, *Monitoring of time between events with a double generally weighted moving average control chart*, Quality and Reliability Engineering International 35 (2019), pp. 685–710.
- [3] M. Anastasopoulou and A.C. Rakitzis, *EWMA control charts for monitoring correlated counts with finite range*, Journal of Applied Statistics (2020), pp. 1–21.
- [4] M. Aslam, M. Azam, and C. Jun, *A new control chart for exponential distributed life using EWMA*, Transactions of the Institute of Measurement and Control 37 (2015), pp. 205–210.
- [5] P. Castagliola, K. Tran, G. Celano, A. Rakitzis, and P. Maravelakis, *An EWMA-type sign chart with exact run length properties*, Journal of Quality Technology 51 (2019), pp. 51–63.
- [6] C.W. Champ, W.H. Woodall, and H.A. Mohsen, *A generalized quality control procedure*, Statistics & probability letters 11 (1991), pp. 211–218.
- [7] Y.S. Chang and D.S. Bai, *Control charts for positively-skewed populations with weighted standard deviations*, Quality and Reliability Engineering International 17 (2001), pp. 397–406.
- [8] F. Gan, *Design of optimal exponential CUSUM control charts*, Journal of Quality Technology 26 (1994), pp. 109–124.
- [9] F. Gan, *Designs of one-and two-sided exponential EWMA charts*, Journal of Quality Technology 30 (1998), pp. 55–69.
- [10] F. Gan and T. Chang, *Computing average run lengths of exponential EWMA charts*, Journal of Quality Technology 32 (2000), pp. 183–187.
- [11] A. Haq, *One-sided and two one-sided MEWMA charts for monitoring process mean*, Journal of Statistical Computation and Simulation 90 (2020), pp. 699–718.
- [12] X. Hu, P. Castagliola, J. Zhong, A. Tang, and Y. Qiao, *On the performance of the adaptive EWMA chart for monitoring time between events*, Journal of Statistical Computation and Simulation (2020), pp. 1–37.
- [13] X. Hu, P. Castagliola, X. Zhou, and A. Tang, *Conditional design of the EWMA median chart with estimated parameters*, Communications in Statistics-Theory and Methods 48 (2019), pp. 1871–1889.
- [14] N. Khan, M. Aslam, and C. Jun, *A EWMA control chart for exponential distributed quality based on moving average statistics*, Quality and Reliability Engineering International 32 (2016), pp. 1179–1190.
- [15] N. Kumar, S. Chakraborti, and A. Rakitzis, *Improved Shewhart-type charts for monitoring times between events*, Journal of Quality Technology 49 (2017), pp. 278–296.
- [16] J.Y. Liu, M. Xie, T.N. Goh, and L. Chan, *A study of EWMA chart with transformed exponential data*, International Journal of Production Research 45 (2007), pp. 743–763.
- [17] M.A. Mahmoud and P.E. Maravelakis, *The performance of the MEWMA control chart when parameters are estimated*, Communications in Statistics-Simulation and Computation 39 (2010), pp. 1803–1817.
- [18] M.S. Nawaz, M. Azam, and M. Aslam, *EWMA and DEWMA repetitive control charts under non-normal processes*, Journal of Applied Statistics 48 (2021), pp. 4–40.
- [19] G. Ozsan, M.C. Testik, and C.H. Weiß, *Properties of the exponential EWMA chart with parameter estimation*, Quality and Reliability Engineering International 26 (2010), pp. 555–569.
- [20] C. Pehlivan and M.C. Testik, *Impact of model misspecification on the exponential EWMA charts: a robustness study when the time-between-events are not exponential*, Quality and Reliability Engineering International 26 (2010), pp. 177–190.

- [21] M.B. Perry, *An EWMA control chart for categorical processes with applications to social network monitoring*, Journal of Quality Technology 52 (2020), pp. 182–197.
- [22] Y. Qiao, X. Hu, J. Sun, and Q. Xu, *Optimal design of one-sided exponential ewma charts with estimated parameters based on the median run length*, IEEE Access 7 (2019), pp. 76645–76658.
- [23] Y. Qiao, J. Sun, P. Castagliola, and X. Hu, *Optimal design of one-sided exponential EWMA charts based on median run length and expected median run length*, Communications in Statistics-Theory and Methods (2020), pp. 1–21.
- [24] L. Qu, M.B. Khoo, P. Castagliola, and Z. He, *Exponential cumulative sums chart for detecting shifts in time-between-events*, International Journal of Production Research 56 (2018), pp. 3683–3698.
- [25] L. Qu, Z. Wu, M.B. Khoo, and P. Castagliola, *A CUSUM scheme for event monitoring*, International Journal of Production Economics 145 (2013), pp. 268–280.
- [26] N.A. Saleh, M.A. Mahmoud, and A.G. Abdel-Salam, *The performance of the adaptive exponentially weighted moving average control chart with estimated parameters*, Quality and Reliability Engineering International 29 (2013), pp. 595–606.
- [27] R.A. Sanusi, S.Y. Teh, and M.B. Khoo, *Simultaneous monitoring of magnitude and time-between-events data with a Max-EWMA control chart*, Computers & Industrial Engineering 142 (2020), p. 106378.
- [28] L. Shu and W. Jiang, *A new EWMA chart for monitoring process dispersion*, Journal of Quality Technology 40 (2008), pp. 319–331.
- [29] L. Shu, W. Jiang, and S. Wu, *A one-sided EWMA control chart for monitoring process means*, Communications in Statistics-Simulation and Computation 36 (2007), pp. 901–920.
- [30] L. Shu, W. Jiang, and Z. Wu, *Exponentially weighted moving average control charts for monitoring increases in Poisson rate*, IIE Transactions 44 (2012), pp. 711–723.
- [31] S. Wu, P. Castagliola, and G. Celano, *A distribution-free EWMA control chart for monitoring time-between-events-and-amplitude data*, Journal of Applied Statistics 48 (2021), pp. 434–454.
- [32] Z. Wu, J. Jiao, and Z. He, *A control scheme for monitoring the frequency and magnitude of an event*, International Journal of Production Research 47 (2009), pp. 2887–2902.
- [33] F. Xie, J. Sun, P. Castagliola, X. Hu, and A. Tang, *A multivariate cusum control chart for monitoring gumbel's bivariate exponential data*, Quality and Reliability Engineering International 37 (2021), pp. 10–33.
- [34] M. Xie, T.N. Goh, V. Kuralmani, and V. Kuralmani, *Statistical Models and Control Charts for High-Quality Processes*, Springer Science & Business Media, 2002.
- [35] J. Yang, H. Yu, Y. Cheng, and M. Xie, *Design of exponential control charts based on average time to signal using a sequential sampling scheme*, International Journal of Production Research 53 (2015), pp. 2131–2145.
- [36] S. Yang and T. Jiang, *Service quality variation monitoring using the interquartile range control chart*, Quality Technology & Quantitative Management 16 (2019), pp. 613–627.
- [37] H.Y. Zhang, M. Shamsuzzaman, M. Xie, and T.N. Goh, *Design and application of exponential chart for monitoring time-between-events data under random process shift*, The International Journal of Advanced Manufacturing Technology 57 (2011), pp. 849–857.
- [38] L. Zhang and G. Chen, *EWMA charts for monitoring the mean of censored Weibull lifetimes*, Journal of Quality Technology 36 (2004), pp. 321–328.
- [39] M. Zhang, F.M. Megahed, and W.H. Woodall, *Exponential CUSUM charts with estimated control limits*, Quality and Reliability Engineering International 30 (2014), pp. 275–286.

Appendix A

Let Y_t be an exponential random variable with scale parameter $\theta = 1$. The p.d.f. and c.d.f. of Y_t are $f_{Y_t}(y) = e^{-y}$ and $F_{Y_t}(y) = 1 - e^{-y}$, respectively. Let us define $Y_t^+ = \max(1, Y_t)$. The p.d.f. $f_{Y_t^+}(y)$ of Y_t^+ is defined on $[1, \infty)$ and it is equal to

$$\begin{aligned} f_{Y_t^+}(y) &= F_{Y_t}(1) \times I_{y=1} + f_{Y_t}(y) \times I_{y>1}, \\ &= (1 - e^{-1}) \times I_{y=1} + e^{-y} \times I_{y>1}, \end{aligned} \quad (\text{A.1})$$

where I is the indicator function. Therefore, the expectation $E(Y_t^+)$ of Y_t^+ is

$$E(Y_t^+) = 1 - e^{-1} + \underbrace{\int_1^{\infty} ye^{-y} dy}_{2e^{-1}}. \quad (\text{A.2})$$

It is not difficult to prove that the integral above is equal to $2e^{-1}$ and we have

$$E(Y_t^+) = 1 + e^{-1}. \quad (\text{A.3})$$

Similarly, the expectation of $(Y_t^+)^2$ is equal to

$$E((Y_t^+)^2) = 1 - e^{-1} + \underbrace{\int_1^\infty y^2 e^{-y} dy}_{5e^{-1}}, \quad (\text{A.4})$$

and since the integral reduces to $5e^{-1}$, we have

$$E((Y_t^+)^2) = 1 + 4e^{-1}. \quad (\text{A.5})$$

Finally, the variance $V(Y_t^+)$ of Y_t^+ can be obtained using

$$\begin{aligned} V(Y_t^+) &= 1 + 4e^{-1} - (1 + e^{-1})^2 = 2e^{-1} - e^{-2} \\ &= e^{-1}(2 - e^{-1}). \end{aligned} \quad (\text{A.6})$$

Now, let us define $Y_t^- = \min(1, Y_t)$. The p.d.f. $f_{Y_t^-}(y)$ of Y_t^- is defined on $[0, 1]$ and it is equal to

$$\begin{aligned} f_{Y_t^-}(y) &= f_{Y_t}(y) \times I_{0 \leq y < 1} + (1 - F_{Y_t}(1)) \times I_{y=1}, \\ &= e^{-y} \times I_{0 \leq y < 1} + e^{-1} \times I_{y=1}. \end{aligned} \quad (\text{A.7})$$

Therefore, the expectation $E(Y_t^-)$ of Y_t^- is equal to

$$E(Y_t^-) = \underbrace{\int_0^1 ye^{-y} dy}_{1-2e^{-1}} + e^{-1}. \quad (\text{A.8})$$

Since the integral above reduces to $1 - 2e^{-1}$, we have

$$E(Y_t^-) = 1 - e^{-1}. \quad (\text{A.9})$$

Note that the expectation of $(Y_t^-)^2$ is equal to

$$E((Y_t^-)^2) = \underbrace{\int_0^1 y^2 e^{-y} dy}_{2-5e^{-1}} + e^{-1}, \quad (\text{A.10})$$

which reduces to

$$E((Y_t^-)^2) = 2 - 4e^{-1}. \quad (\text{A.11})$$

Finally, the variance $V(Y_t^-)$ of Y_t^- can be obtained using

$$\begin{aligned} V(Y_t^-) &= 2 - 4e^{-1} - (1 - e^{-1})^2 = 1 - 2e^{-1} - e^{-2} \\ &= 1 - e^{-1}(2 + e^{-1}). \end{aligned} \quad (\text{A.12})$$

Similar to the known parameter case above, the mean $E(\widehat{Y}_t^+)$ and $E(\widehat{Y}_t^-)$ of the estimated upper- and lower-truncated TBE random variables $\widehat{Y}_t^+ = \max(1, \widehat{Y}_t)$ and $\widehat{Y}_t^- = \min(1, \widehat{Y}_t)$ can also be computed,

respectively, say,

$$E(\widehat{Y}_t^+) = 1 + Ke^{-\frac{1}{K}}, \quad (\text{A.13})$$

$$E(\widehat{Y}_t^-) = K - Ke^{-\frac{1}{K}}, \quad (\text{A.14})$$

where K is defined in (11) as the ratio of the in-control scale parameter θ_0 to its estimator $\widehat{\theta}_0$.

Appendix B

For the proposed lower-sided EWMA TBE scheme with known parameters, the mean and variance of the variable $Y_t^- = \min(1, Y_t)$ are $1 - e^{-1}$ and $1 - e^{-1}(2 + e^{-1})$, respectively. Since the lower-sided EWMA statistic $Q_t^- = rZ_t^- + (1 - r)Q_{t-1}^- \leq \frac{1}{1 - e^{-1}}$, the in-control region is defined as $[H^-, \frac{1}{1 - e^{-1}}]$, and then the width of each subinterval $w^- = \frac{1/(1 - e^{-1}) - H^-}{M}$ can be obtained. The midpoint value of the i th subinterval is $L_i^- = \frac{1}{1 - e^{-1}} - (i - 0.5)w^-$, where $i = 1, 2, \dots, M$. Based on that, the transition probability $q_{i,j}$ of the charting statistic Q_t^- from state i to state j is given as follow,

$$\begin{aligned} q_{i,j} &= \Pr(Q_t^- \in \text{state } j \mid Q_{t-1}^- \in \text{state } i) \\ &= \Pr\left(1 - \frac{(1 - e^{-1})[j - (1 - r)(i - 0.5)]w^-}{r} < Y_t^- \right. \\ &\quad \left. \leq 1 - \frac{(1 - e^{-1})[j - 1 - (1 - r)(i - 0.5)]w^-}{r}\right). \end{aligned} \quad (\text{B.1})$$

Similarly, let us define

$$A_3 = 1 - \frac{(1 - e^{-1})[j - (1 - r)(i - 0.5)]w^-}{r}, \quad (\text{B.2})$$

$$A_4 = 1 - \frac{(1 - e^{-1})[j - 1 - (1 - r)(i - 0.5)]w^-}{r}. \quad (\text{B.3})$$

Then, the elements $q_{i,j}$ can be obtained using,

$$q_{i,j} = \begin{cases} 0, & \text{if } A_3 > 1 \\ 1 - F_S\left(\frac{A_3}{c}\right), & \text{if } A_3 \leq 1 \text{ and } A_4 > 1 \\ F_S\left(\frac{A_4}{c}\right) - F_S\left(\frac{A_3}{c}\right), & \text{if } A_3 \leq 1 \text{ and } A_4 \leq 1 \end{cases} \quad (\text{B.4})$$

Meanwhile, the elements p_j of vector \mathbf{p} are,

$$p_j = \begin{cases} 1, & L_j^- - \frac{w^-}{2} < Q_0^- < L_j^- + \frac{w^-}{2} \\ 0, & \text{otherwise} \end{cases} \quad (\text{B.5})$$

where $Q_0^- = 1$. By using (24) and (25), one can easily compute the ARL and SDRL values of the proposed lower-sided EWMA TBE chart with known parameters, respectively.

For the parameter estimation case, we characterize the conditional $\widehat{\text{ARL}}$ and $\widehat{\text{SDRL}}$ as functions of the mean shift c and conditional on the fixed value of k , i.e., $\widehat{\text{ARL}}(c|k)$ and $\widehat{\text{SDRL}}(c|k)$, respectively (see [19]). Based on this, the unconditional $\widehat{\text{ARL}}$ value of the proposed one-sided EWMA TBE chart can be computed

by integrating the conditional $\widehat{\text{ARL}}(c|k)$ value with respect to k , say,

$$\begin{aligned}\widehat{\text{ARL}} &= \int_0^{+\infty} \widehat{\text{ARL}}(c|k) f_K(k|m) dk \\ &= \int_0^{+\infty} \widehat{\mathbf{p}}^\top (\mathbf{I} - \widehat{\mathbf{Q}})^{-1} \mathbf{1} f_K(k|m) dk.\end{aligned}\quad (\text{B.6})$$

Also, the corresponding unconditional $\widehat{\text{SDRL}}$ value can be obtained using,

$$\begin{aligned}\widehat{\text{SDRL}} &= \int_0^{+\infty} \widehat{\text{SDRL}}(c|k) f_K(k|m) dk \\ &= \int_0^{+\infty} \sqrt{2\widehat{\mathbf{p}}^\top (\mathbf{I} - \widehat{\mathbf{Q}})^{-2} \widehat{\mathbf{Q}} \mathbf{1} - (\widehat{\text{ARL}})^2 + \widehat{\text{ARL}}} \\ &\quad \times f_K(k|m) dk,\end{aligned}\quad (\text{B.7})$$

where $f_K(k|m)$ is defined in (12). Moreover, the conditional transition probability matrix $\widehat{\mathbf{Q}} = [\widehat{q}_{i,j}]_{M \times M}$ can be computed as follow:

- Because the mean $E(\widehat{Y}_t^+)$ of the estimated variable $\widehat{Y}_t^+ = \max(1, \widehat{Y}_t)$ is equal to $1 + Ke^{-\frac{1}{k}}$, and the scaling of the estimated variable \widehat{Y}_t^+ is defined as $\widehat{Z}^+ = \widehat{Y}_t^+ / (1 + Ke^{-\frac{1}{k}})$. Similar to the known parameter case, the elements $\widehat{q}_{i,j}$ can be obtained as follow,

$$\begin{aligned}\widehat{q}_{i,j} &= \Pr\left(\widehat{Q}_t^+ \in \text{state } j \mid \widehat{Q}_{t-1}^+ \in \text{state } i\right) \\ &= \Pr\left(1 + \frac{(1 + ke^{-\frac{1}{k}})[j - 1 - (1 - r)(i - 0.5)] \widehat{w}^+}{r}\right. \\ &\quad \left. < \widehat{Y}_t^+ \leq 1 + \frac{(1 + ke^{-\frac{1}{k}})[j - (1 - r)(i - 0.5)] \widehat{w}^+}{r}\right).\end{aligned}\quad (\text{B.8})$$

where $\widehat{w}^+ = \frac{1}{M} \left(\widehat{H}^+ - 1 / (1 + ke^{-\frac{1}{k}}) \right)$, and \widehat{H}^+ is the control limit of the proposed upper-sided EWMA TBE chart with estimated parameters. Then, let us define

$$\widehat{A}_1 = 1 + \frac{(1 + ke^{-\frac{1}{k}})[j - 1 - (1 - r)(i - 0.5)] \widehat{w}^+}{r}, \quad (\text{B.9})$$

$$\widehat{A}_2 = 1 + \frac{(1 + ke^{-\frac{1}{k}})[j - (1 - r)(i - 0.5)] \widehat{w}^+}{r}. \quad (\text{B.10})$$

The entire $\widehat{q}_{i,j}$ can be obtained as follow,

$$\widehat{q}_{i,j} = \begin{cases} 0, & \text{if } \widehat{A}_2 < 1 \\ F_S\left(\frac{\widehat{A}_2}{kc}\right), & \text{if } \widehat{A}_2 \geq 1 \text{ and } \widehat{A}_1 < 1 \\ F_S\left(\frac{\widehat{A}_2}{kc}\right) - F_S\left(\frac{\widehat{A}_1}{kc}\right), & \text{if } \widehat{A}_2 \geq 1 \text{ and } \widehat{A}_1 \geq 1 \end{cases} \quad (\text{B.11})$$

Meanwhile, the elements \widehat{p}_j of vector $\widehat{\mathbf{p}}$ are,

$$\widehat{p}_j = \begin{cases} 1, & \widehat{L}_j^+ - \frac{\widehat{w}^+}{2} < \widehat{Q}_0^+ < \widehat{L}_j^+ + \frac{\widehat{w}^+}{2} \\ 0, & \text{otherwise} \end{cases} \quad (\text{B.12})$$

where $\widehat{L}_j^+ = 1/(1 + ke^{-\frac{1}{k}}) + (j - 0.5)\widehat{w}^+$, and $\widehat{Q}_0^+ = 1$.

- For the proposed lower-sided EWMA TBE scheme with estimated parameters, the corresponding transient probabilities $\widehat{q}_{i,j}$ can be obtained using $\widehat{Z}^- = \widehat{Y}_t^- / (K - Ke^{-\frac{1}{k}})$, i.e.,

$$\begin{aligned}\widehat{q}_{i,j} &= \Pr\left(\widehat{Q}_t^- \in \text{state } j \mid \widehat{Q}_{t-1}^- \in \text{state } i\right) \\ &= \Pr\left(1 - \frac{(k - ke^{-\frac{1}{k}})[j - (1-r)(i-0.5)]\widehat{w}^-}{r} < \widehat{Y}_t^- \right. \\ &\quad \left. \leq 1 - \frac{(k - ke^{-\frac{1}{k}})[j - 1 - (1-r)(i-0.5)]\widehat{w}^-}{r}\right).\end{aligned}\tag{B.13}$$

where $\widehat{w}^- = \frac{1}{M} \left(1/(k - ke^{-\frac{1}{k}}) - \widehat{H}^-\right)$, and \widehat{H}^- is the control limit of the suggested lower-sided EWMA TBE chart with estimated parameters. Let

$$\widehat{A}_3 = 1 - \frac{(k - ke^{-\frac{1}{k}})[j - (1-r)(i-0.5)]\widehat{w}^-}{r},\tag{B.14}$$

$$\widehat{A}_4 = 1 - \frac{(k - ke^{-\frac{1}{k}})[j - 1 - (1-r)(i-0.5)]\widehat{w}^-}{r}.\tag{B.15}$$

Then, the elements $\widehat{q}_{i,j}$ are,

$$\widehat{q}_{i,j} = \begin{cases} 0, & \text{if } \widehat{A}_3 > 1 \\ 1 - F_S\left(\frac{\widehat{A}_3}{kc}\right), & \text{if } \widehat{A}_3 \leq 1 \text{ and } \widehat{A}_4 > 1 \\ F_S\left(\frac{\widehat{A}_4}{kc}\right) - F_S\left(\frac{\widehat{A}_3}{kc}\right), & \text{if } \widehat{A}_3 \leq 1 \text{ and } \widehat{A}_4 \leq 1 \end{cases}\tag{B.16}$$

Also, the elements \widehat{p}_j of vector $\widehat{\mathbf{p}}$ can be obtained using,

$$\widehat{p}_j = \begin{cases} 1, & \widehat{L}_j^- - \frac{\widehat{w}^-}{2} < \widehat{Q}_0^- < \widehat{L}_j^- + \frac{\widehat{w}^-}{2} \\ 0, & \text{otherwise} \end{cases}\tag{B.17}$$

where $\widehat{Q}_0^- = 1$ and $\widehat{L}_j^- = 1/(k - ke^{-\frac{1}{k}}) - (j - 0.5)\widehat{w}^-$.

In this paper, the Gauss-Legendre quadrature can be used to overcome the computational difficulties caused by (B.6) and (B.7) so as to obtain an approximation of these integrals.

Table 1.: Control limits of the upper-sided EWMA TBE and upper-sided REWMA charts for $ARL_0 \in \{200, 370, 500\}$, $r(\lambda_Q) \in \{0.03, 0.05, 0.07, 0.1, 0.2, 0.3, 0.4, 0.5, 0.6, 0.7, 0.8, 0.9\}$ and $m \in \{50, 200, 1000, +\infty\}$.

ARL ₀	Charts	m	r(λ _Q)												
			0.03	0.05	0.07	0.1	0.2	0.3	0.4	0.5	0.6	0.7	0.8	0.9	
200	Proposed	10	1.0986	1.1576	1.2133	1.2935	1.5486	1.7975	2.0444	2.2915	2.5396	2.7893	3.0406	3.2938	
		50	1.1122	1.1814	1.2457	1.3370	1.6209	1.8943	2.1646	2.4348	2.7063	2.9802	3.2565	3.5354	
		200	1.1142	1.1848	1.2505	1.3436	1.6322	1.9097	2.1836	2.4575	2.7328	3.0105	3.2907	3.5737	
		+∞	1.1148	1.1860	1.2521	1.3456	1.6359	1.9147	2.1897	2.4648	2.7413	3.0202	3.3017	3.5861	
	Existing	10	1.1109	1.1824	1.2522	1.3546	1.6820	1.9970	2.3056	2.6106	2.9135	3.2153	3.5164	3.8171	
		50	1.1982	1.3096	1.4122	1.5557	1.9878	2.3873	2.7731	3.1523	3.5285	3.9034	4.2780	4.6526	
		200	1.2387	1.3601	1.4697	1.6210	2.0716	2.4862	2.8863	3.2797	3.6701	4.0596	4.4490	4.8387	
		+∞	1.2565	1.3809	1.4924	1.6460	2.1020	2.5214	2.9262	3.3243	3.7195	4.1138	4.5082	4.9031	
370	Proposed	10	1.1205	1.1869	1.2499	1.3409	1.6312	1.9153	2.1972	2.4798	2.7635	3.0491	3.3364	3.6257	
		50	1.1446	1.2239	1.2974	1.4015	1.7260	2.0395	2.3500	2.6610	2.9738	3.2896	3.6080	3.9295	
		200	1.1477	1.2291	1.3042	1.4104	1.7406	2.0587	2.3736	2.6891	3.0064	3.3268	3.6501	3.9766	
		+∞	1.1487	1.2307	1.3064	1.4133	1.7452	2.0649	2.3812	2.6981	3.0169	3.3387	3.6636	3.9916	
	Existing	10	1.1215	1.1998	1.2765	1.3890	1.7506	2.1002	2.4438	2.7843	3.1231	3.4610	3.7984	4.1355	
		50	1.2251	1.3503	1.4654	1.6263	2.1119	2.5633	3.0010	3.4326	3.8618	4.2902	4.7189	5.1479	
		200	1.2784	1.4150	1.5379	1.7076	2.2145	2.6840	3.1393	3.5886	4.0357	4.4825	4.9299	5.3781	
		+∞	1.3032	1.4426	1.5673	1.7391	2.2521	2.7273	3.1883	3.6434	4.0966	4.5495	5.0033	5.4580	
500	Proposed	10	1.1293	1.1992	1.2657	1.3620	1.6693	1.9704	2.2694	2.5691	2.8701	3.1730	3.4778	3.7845	
		50	1.1595	1.2436	1.3213	1.4316	1.7760	2.1091	2.4395	2.7706	3.1038	3.4402	3.7794	4.1219	
		200	1.1633	1.2496	1.3292	1.4418	1.7922	2.1304	2.4655	2.8015	3.1397	3.4811	3.8256	4.1735	
		+∞	1.1645	1.2515	1.3317	1.4450	1.7973	2.1371	2.4739	2.8114	3.1511	3.4942	3.8404	4.1901	
	Existing	10	1.1263	1.2078	1.2876	1.4049	1.7823	2.1482	2.5084	2.8656	3.2213	3.5762	3.9307	4.2850	
		50	1.2373	1.3689	1.4898	1.6590	2.1705	2.6471	3.1102	3.5675	4.0227	4.4773	4.9323	5.3879	
		200	1.2967	1.4405	1.5697	1.7482	2.2825	2.7790	3.2614	3.7383	4.2133	4.6884	5.1643	5.6413	
		+∞	1.3251	1.4714	1.6024	1.7831	2.3238	2.8264	3.3151	3.7985	4.2802	4.7622	5.2452	5.7294	

Table 2.: (ARL₁, SDRL₁) profiles of the upper-sided EWMA TBE and upper-sided REWMA charts when ARL₀ = 500.

c	Charts	r(λ _Q)	r(λ _Q)												
			0.03	0.05	0.07	0.1	0.2	0.3	0.4	0.5	0.6	0.7	0.8	0.9	
1.05	Proposed	<i>h</i> ⁺	1.1645	1.2515	1.3317	1.4450	1.7973	2.1371	2.4739	2.8114	3.1511	3.4942	3.8404	4.1900	
		<i>h</i> _Q	1.3251	1.4714	1.6024	1.7831	2.3238	2.8264	3.3151	3.7985	4.2802	4.7622	5.2452	5.7294	
1.1	Proposed	<i>h</i> ⁺	(267.60, 258.83)	(283.83, 277.27)	(295.34, 290.32)	(307.83, 304.19)	(331.97, 330.25)	(344.95, 343.84)	(353.39, 352.56)	(359.12, 358.45)	(363.29, 362.70)	(366.44, 365.89)	(368.79, 368.27)	(370.55, 370.04)	
		<i>h</i> _Q	(285.41, 269.18)	(297.51, 286.73)	(306.83, 298.82)	(317.15, 311.45)	(337.21, 334.45)	(348.28, 346.54)	(355.44, 354.19)	(360.49, 359.52)	(364.12, 363.33)	(366.90, 366.22)	(369.00, 368.40)	(370.62, 370.07)	
1.3	Proposed	<i>h</i> ⁺	(163.89, 153.20)	(178.36, 170.61)	(189.60, 183.72)	(202.81, 198.58)	(230.82, 228.85)	(247.24, 246.00)	(258.31, 257.40)	(266.11, 265.39)	(271.90, 271.28)	(276.31, 275.75)	(279.67, 279.13)	(282.21, 281.70)	
		<i>h</i> _Q	(179.96, 164.03)	(191.67, 180.90)	(201.36, 193.29)	(212.83, 207.05)	(237.09, 234.27)	(251.41, 249.63)	(261.02, 259.74)	(267.93, 266.95)	(273.03, 272.23)	(276.95, 276.27)	(279.96, 279.36)	(282.31, 281.76)	
1.5	Proposed	<i>h</i> ⁺	(50.31, 40.41)	(53.81, 46.07)	(57.34, 51.10)	(62.45, 57.70)	(76.74, 74.32)	(87.49, 85.96)	(95.75, 94.66)	(102.18, 101.33)	(107.27, 106.57)	(111.33, 110.72)	(114.57, 114.01)	(117.13, 116.61)	
		<i>h</i> _Q	(56.07, 43.06)	(58.65, 49.14)	(61.87, 54.41)	(66.71, 61.11)	(80.20, 77.31)	(90.17, 88.31)	(97.72, 96.38)	(103.60, 102.57)	(108.22, 107.38)	(111.91, 111.20)	(114.85, 114.24)	(117.22, 116.67)	
1.7	Proposed	<i>h</i> ⁺	(27.26, 19.73)	(28.05, 21.82)	(29.11, 23.84)	(30.96, 26.71)	(37.26, 34.85)	(42.85, 41.25)	(47.57, 46.41)	(51.49, 50.59)	(54.75, 54.01)	(57.47, 56.83)	(59.70, 59.13)	(61.52, 60.99)	
		<i>h</i> _Q	(30.51, 20.45)	(30.49, 22.70)	(31.26, 24.89)	(32.90, 27.91)	(38.93, 36.15)	(44.25, 42.40)	(48.67, 47.33)	(52.33, 51.29)	(55.35, 54.50)	(57.84, 57.13)	(59.90, 59.28)	(61.59, 61.03)	
2	Proposed	<i>h</i> ⁺	(18.43, 12.56)	(18.50, 13.50)	(18.81, 14.46)	(19.54, 15.90)	(22.60, 20.34)	(25.68, 24.11)	(28.48, 27.30)	(30.91, 29.99)	(33.02, 32.26)	(34.83, 34.18)	(36.36, 35.78)	(37.64, 37.10)	
		<i>h</i> _Q	(20.83, 12.85)	(20.19, 13.81)	(20.21, 14.84)	(20.73, 16.38)	(23.55, 20.96)	(26.49, 24.71)	(29.14, 27.81)	(31.44, 30.40)	(33.40, 32.56)	(35.08, 34.36)	(36.50, 35.87)	(37.68, 37.13)	
3	Proposed	<i>h</i> ⁺	(12.41, 8.06)	(12.20, 8.41)	(12.17, 8.81)	(12.35, 9.44)	(13.55, 11.57)	(15.00, 13.54)	(16.42, 15.28)	(17.73, 16.82)	(18.92, 18.15)	(19.97, 19.31)	(20.90, 20.30)	(21.69, 21.15)	
		<i>h</i> _Q	(14.23, 8.22)	(13.44, 8.52)	(13.16, 8.93)	(13.13, 9.59)	(14.09, 11.81)	(15.44, 13.79)	(16.78, 15.52)	(18.03, 17.02)	(19.14, 18.30)	(20.13, 19.41)	(20.98, 20.36)	(21.72, 21.16)	
5	Proposed	<i>h</i> ⁺	(6.17, 3.83)	(5.93, 3.84)	(5.80, 3.88)	(5.71, 3.97)	(5.76, 4.40)	(5.99, 4.87)	(6.29, 5.33)	(6.59, 5.76)	(6.90, 6.17)	(7.19, 6.53)	(7.46, 6.87)	(7.71, 7.16)	
		<i>h</i> _Q	(7.25, 3.98)	(6.68, 3.92)	(6.39, 3.94)	(6.16, 4.01)	(6.01, 4.43)	(6.17, 4.91)	(6.42, 5.37)	(6.70, 5.80)	(6.98, 6.20)	(7.25, 6.88)	(7.50, 6.88)	(7.73, 7.17)	
8	Proposed	<i>h</i> ⁺	(3.42, 2.09)	(3.28, 2.05)	(3.19, 2.04)	(3.11, 2.03)	(3.03, 2.09)	(3.04, 2.19)	(3.08, 2.30)	(3.14, 2.42)	(3.20, 2.53)	(3.27, 2.64)	(3.34, 2.74)	(3.40, 2.84)	
		<i>h</i> _Q	(4.04, 2.24)	(3.72, 2.15)	(3.54, 2.11)	(3.38, 2.09)	(3.18, 2.12)	(3.14, 2.21)	(3.15, 2.32)	(3.19, 2.43)	(3.24, 2.54)	(3.29, 2.65)	(3.35, 2.75)	(3.41, 2.84)	
10	Proposed	<i>h</i> ⁺	(2.34, 1.39)	(2.25, 1.35)	(2.20, 1.33)	(2.15, 1.31)	(2.08, 1.31)	(2.06, 1.33)	(2.06, 1.36)	(2.08, 1.40)	(2.09, 1.44)	(2.11, 1.48)	(2.13, 1.52)	(2.15, 1.56)	
		<i>h</i> _Q	(2.72, 1.52)	(2.52, 1.45)	(2.42, 1.40)	(2.32, 1.37)	(2.17, 1.34)	(2.12, 1.35)	(2.11, 1.38)	(2.11, 1.41)	(2.11, 1.45)	(2.13, 1.49)	(2.14, 1.53)	(2.16, 1.56)	

Table 9.: The simulated dataset for Example 1
 $(\theta_0 = 10, \theta_1 = 18 \text{ and } c = 1.8)$.

t	X_t	EWMA TBE		REWMA	
		Y_t^+	Q_t^+	Y_t	Q_t
1	20.8057	2.0806	1.4391	2.0806	1.1081
2	5.7453	1.0000	1.3952	0.5745	1.0547
3	11.9176	1.1918	1.3749	1.1918	1.0684
4	4.2283	1.0000	1.3374	0.4228	1.0039
5	28.5700	2.8570	1.4894	2.8570	1.1892
6	6.9921	1.0000	1.4404	0.6992	1.1402
7	53.0499	5.3050	1.8269	5.3050	1.5567
8	3.9902	1.0000	1.7442	0.3990	1.4409
9	6.9799	1.0000	1.6698	0.6980	1.3666
10	0.9991	1.0000	1.6028	0.0999	1.2399
11	43.0341	4.3034	1.8729	4.3034	1.5463
12	1.7285	1.0000	1.7856	0.1729	1.4089
13	12.1219	1.2122	1.7282	1.2122	1.3893
14	8.7532	1.0000	1.6554	0.8753	1.3379
15	20.7322	2.0732	1.6972	2.0732	1.4114
16	46.0375	4.6037	1.9878	4.6037	1.7306
17	2.9123	1.0000	1.8891	0.2912	1.5867
18	34.8172	3.4817	2.0483	3.4817	1.7762
19	17.8729	1.7873	2.0222	1.7873	1.7773
20	8.5353	1.0000	1.9200	0.8535	1.6849
21	0.0441	1.0000	1.8280	0.0044	1.5169
22	11.8628	1.1863	1.7638	1.1863	1.4838
23	0.1716	1.0000	1.6874	0.0172	1.3372
24	26.7274	2.6727	1.7860	2.6727	1.4707
25	16.5832	1.6583	1.7732	1.6583	1.4895
26	6.5086	1.0000	1.6959	0.6509	1.4056
27	49.3004	4.9300	2.0193	4.9300	1.7581
28	5.2345	1.0000	1.9174	0.5234	1.6346
29	15.5979	1.5598	1.8816	1.5598	1.6271
30	3.7637	1.0000	1.7935	0.3764	1.5020

Table 10.: Time between consecutive accidents of F-16 aircraft
 $(\theta_0 = 1460, \theta_1 = 615 \text{ and } c = 0.4212)$.

t	X_t	EWMA TBE		REWMA	
		Y_t^-	Q_t^-	Y_t	q_t
1	1456	0.9973	0.6431	0.9973	0.9999
2	231	0.1582	0.6285	0.1582	0.9747
3	691	0.4733	0.6239	0.4733	0.9596
4	122	0.0836	0.6077	0.0836	0.9333
5	718	0.4918	0.6042	0.4918	0.9201
6	1147	0.7856	0.6096	0.7856	0.9161
7	225	0.1541	0.5960	0.1541	0.8932
8	706	0.4836	0.5926	0.4836	0.8809
9	499	0.3418	0.5851	0.3418	0.8647
10	587	0.4021	0.5796	0.4021	0.8509
11	561	0.3842	0.5737	0.3842	0.8369
12	547	0.3747	0.5677	0.3747	0.8230
13	448	0.3068	0.5599	0.3068	0.8075
14	1561	1.0000	0.5731	1.0692	0.8154
15	53	0.0363	0.5570	0.0363	0.7920
16	280	0.1918	0.5461	0.1918	0.7740

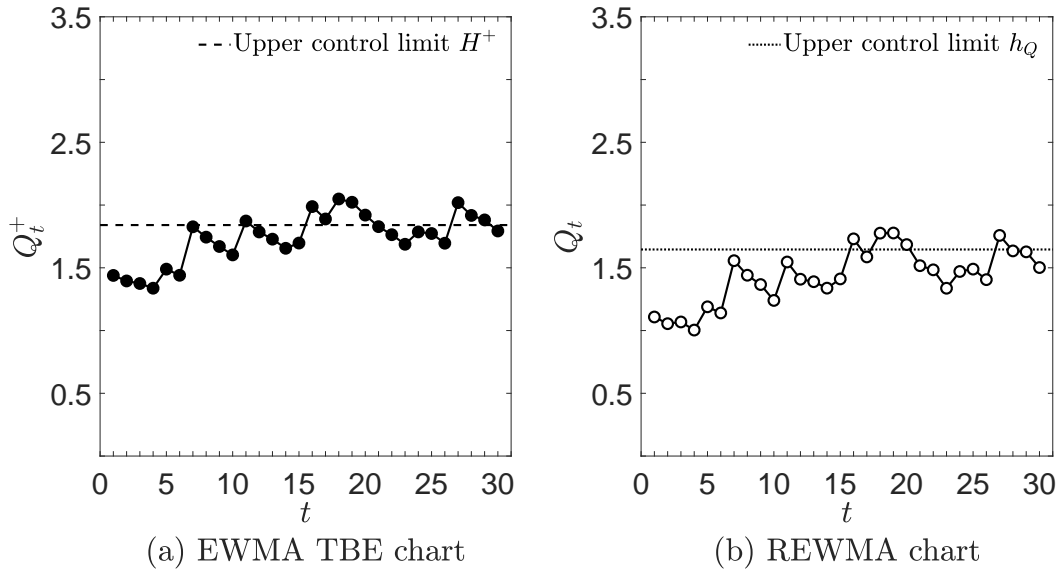


Figure 1.: The (a) upper-sided EWMA TBE chart and (b) upper-sided REWMA chart for the data in Table 9 ($r = 0.1, H^+ = 1.8406, h_Q = 1.6460$).

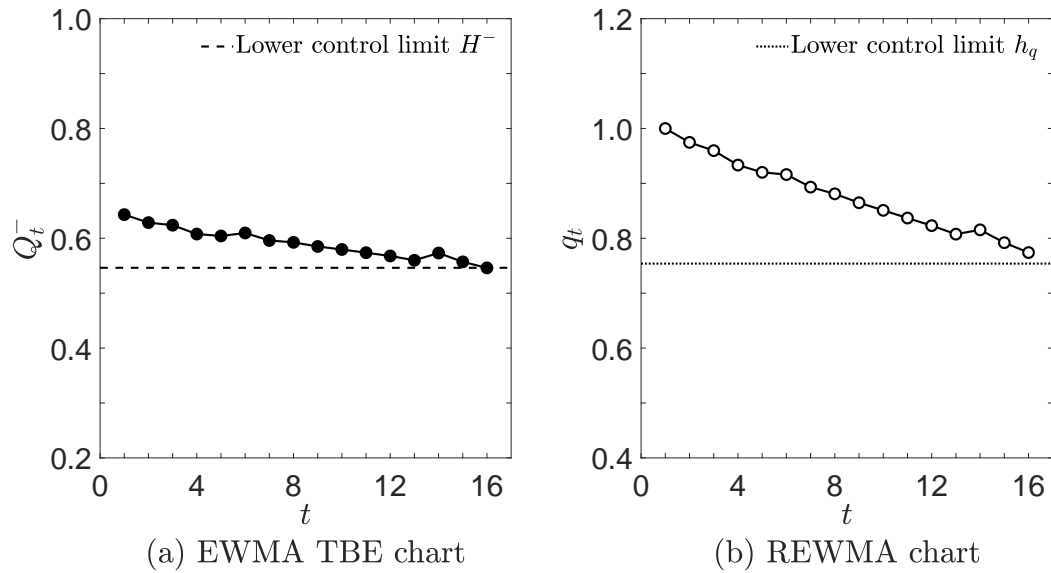


Figure 2.: The (a) lower-sided EWMA TBE chart and (b) lower-sided REWMA chart for the data in Table 10 ($r = 0.03, H^- = 0.5462, h_q = 0.7539$).